

Stability of fermionic gases close to a p -wave Feshbach resonance

J. Levinsen,¹ N. R. Cooper,² and V. Gurarie³

¹*Laboratoire Physique Théorique et Modèles Statistique, Université Paris Sud, CNRS, 91405 Orsay, France*

²*TCM Group, Cavendish Laboratory, J. J. Thomson Avenue, Cambridge CB3 0HE, United Kingdom*

³*Department of Physics, University of Colorado, Boulder, Colorado 80309, USA*

(Received 6 September 2008; published 22 December 2008)

We study the stability of the paired fermionic p -wave superfluid made out of identical atoms all in the same hyperfine state close to a p -wave Feshbach resonance. First we reproduce known results concerning the lifetime of a three-dimensional superfluid, in particular, we show that it decays at the same rate as its interaction energy, which may preclude its equilibration before it decays. Then we proceed to study its stability in the case when the superfluid is confined to two dimension (2D) by means of an optical harmonic potential. We find that the relative stability is improved in 2D in the BCS regime, such that the decay rate is now parametrically slower than the appropriate interaction energy scale, leading to the possibility of an equilibrated p -wave superfluid in 2D.

DOI: 10.1103/PhysRevA.78.063616

PACS number(s): 03.75.Ss, 74.20.Rp, 34.50.-s

I. INTRODUCTION

Recent success of BEC-BCS crossover experiments in atomic fermionic gases with s -wave Feshbach resonances [1–3] inspired studies towards creating p -wave fermionic superfluids using p -wave Feshbach resonances [4–7]. A number of features made the p -wave superfluids attractive, as discussed at length in Ref. [8]. First of all, it is sufficient to put atoms into identical hyperfine states to suppress their s -wave scattering, leaving p -wave scattering as the strongest scattering channel. Indeed, p -wave Feshbach resonances between atoms in identical hyperfine states were identified and studied some time ago [9,10]. Next, the p -wave superfluids display a number of features distinguishing them from their s -wave counterparts. A richer p -wave order parameter allows for a possibility of observing different phases of the p -wave superfluids, some of which are akin to the phases of superfluid Helium III [11]. Chiral and polar phases of the p -wave condensates are possible, differing by the projection of the angular momentum of the Cooper pairs (or molecules) of the condensate onto the chosen axis. If this projection is ± 1 , the condensate is called chiral, while if it is 0 the condensate is called polar. Another important feature is that as the system is tuned from BCS to BEC, it does not go through a crossover as in the s -wave case, rather it goes through a phase transition as first discussed by Volovik in Ref. [12], long before current experiments on the BCS-BEC systems became possible. Thus the BCS and Bose-Einstein condensate (BEC) are two distinct phases of p -wave condensates (with either of them possibly being chiral or polar, bringing the total number of phases to four). Finally, when confined to two dimensions (2D), the chiral BCS phase of the p -wave superfluids is topological and its vortices have trapped quasiparticles which obey non-Abelian statistics [13,14]. Such quasiparticles have been suggested to be used as topologically protected qubits to construct decoherence free quantum computers [15].

However, the program to create these superfluids suffered a setback when experimental studies of the p -wave Feshbach molecules showed they were unstable, with the lifetime vary-

ing between 2 and 20 ms [16–19]. Although some of these studies were done with molecules made of atoms of ^{40}K , which are inherently unstable due to dipolar relaxation [17], the rest of the studies used atoms of ^6Li , whose p -wave molecules should not, by themselves, exhibit any instability.

A common mechanism which can lead to instability in atomic gases is the atom-molecule and molecule-molecule relaxation [20]. This is the process which, for example, involves one of the atoms approaching a molecule, with the result being that the molecule collapses into one of its strongly bound states, while the excess energy is carried away by the atom. Such processes are suppressed in the s -wave superfluid due to the Pauli principle, as was convincingly demonstrated in Refs. [20,21]. However, the Pauli principle does not protect the p -wave superfluids, potentially leading to much shorter lifetimes.

References [22,23] examined the stability of the p -wave condensates due to these relaxation processes, as well as due to a possible recombination into trimers [22–24]. In [22], we established that the decay rate of a condensate of p -wave molecules close to Feshbach resonance is given by

$$\Gamma_{3\text{D}} \sim \frac{\hbar}{m\ell^2} \frac{R_e}{\ell}, \quad (1)$$

where ℓ is the typical interatomic spacing and R_e is the van der Waals length (the interaction range), typically estimated to be ~ 50 a.u. (so the ratio ℓ/R_e , assuming that $\ell \sim 10\,000$ a.u., is of order 200). $\hbar^2/(m\ell^2)$ is the Fermi energy of the gas. Thus for a gas of Fermi energy about 10 KHz, this gives an estimated lifetime of $1/\Gamma \sim 20$ ms, which is not far from what is measured experimentally. This should be compared with the corresponding expression for the decay rate of the s -wave condensate,

$$\Gamma_{s\text{-wave}} \sim \frac{\hbar}{m\ell^2} \left(\frac{R_e}{\ell} \right)^{3.55}, \quad (2)$$

which is orders of magnitude slower than the p -wave rate, leading to a stable condensate.

The calculations leading to the expression, Eq. (1), were done solely in three-dimensional (3D) space. Yet the most interesting p -wave condensate, the one with non-Abelian quasiparticles, must be confined to two dimensions. The confinement may affect the lifetime of the condensate. In the absence of any experiments in which the p -wave resonant gases are confined to 2D, it is imperative that a theoretical calculation is done estimating this lifetime.

In this paper we estimate the lifetime of the p -wave condensates close to Feshbach resonance confined to 2D. For purely 2D condensates we find that their decay rate is given by

$$\Gamma_{2D} \sim \frac{\hbar}{m\ell^2}. \quad (3)$$

This is even faster than the 3D case, Eq. (1). However, for the quasi-2D condensates, the ones which are confined to a ‘‘pancake’’ of width d , where $d \ll \ell$ and at the same time $d \gg R_e$, we find that the decay rate is given by

$$\Gamma_{\text{quasi-2D}} \sim \frac{\hbar R_e}{m\ell^2 d}. \quad (4)$$

Notice that this expression interpolates between Eqs. (1) and (3). Indeed, as d becomes smaller than ℓ , Eq. (1) gets replaced by Eq. (4). As d is decreased, it eventually becomes smaller than R_e , at which point Eq. (4) gets replaced by Eq. (3).

The rate in the quasi-2D geometry, given by Eq. (4) is somewhat faster than the 3D rate, Eq. (1). So one may jump to the conclusion that the quasi-2D geometry in fact decreases the lifetime of the condensate. This however must be contrasted with the fact that in 2D the interactions are stronger. Indeed, the typical interaction energy per particle of the 3D condensate (assuming that it is in the ‘‘strong’’ resonance regime [22] and concentrating, for simplicity, on the BCS regime only) is

$$E_{3D} \sim \frac{\hbar^2 R_e}{m\ell^2 \ell}, \quad (5)$$

which is of the same order as Γ_{3D} from Eq. (1). Thus, the condensate decays in 3D as fast as it interacts. On the other hand, in 2D the interaction energy is given by

$$E_{2D} \sim \frac{\hbar^2}{m\ell^2} \frac{1}{\ln\left(\frac{\ell}{R_e}\right)}. \quad (6)$$

Comparing this result with Γ_{2D} from Eq. (3), we see that the interaction energy is weaker than the decay rate, by a logarithmic factor.

However, the case we are interested in is quasi-2D, when the condensate is confined to a pancake of width d . Under these conditions, the decay rate is given by Eq. (4), while the interaction strength is still given by Eq. (6), with d substituted for R_e . Provided that

$$\frac{1}{\ln\left(\frac{\ell}{d}\right)} \gg \frac{R_e}{d}, \quad (7)$$

the interaction energy in quasi-2D can be larger than the decay rate, thus creating a situation where the condensate might have sufficient time to form. In turn, since $d \gg R_e$ and logarithms, even of large arguments, are typically not very large, Eq. (7) may indeed hold. The fact that the quasi-2D BCS p -wave condensates are more stable than their 3D counterparts is the main conclusion of this paper.

The rest of the paper is organized as follows.

In Sec. II we go over the analysis of the stability of the 3D p -wave superfluid, mostly following discussions in Ref. [22]. In particular, in Sec. II A we study the two-channel model describing the superfluid and explain the difference between strong and weak resonances, as well as narrow and wide ones, while in Sec. II B we go over the stability analysis.

In Sec. III we present the analysis of the stability in 2D. First, in Sec. III A we set up a 2D p -wave gas. Next, in Sec. III B we discuss the stability of the condensates when the molecules are large, relevant in 3D s -wave and 2D p -wave cases. In the next Sec. III C we set up the three-body problem which needs to be solved to compute the decay rate. In Sec. III D this problem is solved. Finally, in Sec. III E the implications of the solution are discussed and the decay rate is derived. Sections III A and III D are the most technically involved parts of the paper and can be safely omitted at first reading.

In Sec. IV, we go over the analysis in quasi-2D, where the condensate is confined to a pancake geometry. This section is followed by Conclusions and two Appendixes.

Our final remark concerns the usage of the Planck constant \hbar . It generally helps to omit it in calculations because it clutters the expressions and makes them harder to manipulate, while it can always be restored everywhere by dimensional analysis. So we adopt notations where $\hbar=1$ everywhere in this paper from here on.

II. STABILITY OF THE 3D p -WAVE FERMIONIC SUPERFLUID

A. Two-channel model

To describe the 3D p -wave resonantly coupled superfluid we employ a two-channel model with Hamiltonian [6–8,25–27]

$$H = \sum_{\mathbf{p}} \frac{p^2}{2m} \hat{a}_{\mathbf{p}}^{\dagger} \hat{a}_{\mathbf{p}} + \sum_{\mathbf{q}, \mu} \left(\epsilon_0 + \frac{q^2}{4m} \right) \hat{b}_{\mu\mathbf{q}}^{\dagger} \hat{b}_{\mu\mathbf{q}} + \sum_{\mathbf{p}, \mathbf{q}, \mu} \frac{g(|\mathbf{p}|)}{\sqrt{V}} (\hat{b}_{\mu\mathbf{q}} \hat{a}_{\mathbf{p}}^{\dagger} \hat{a}_{\mathbf{q}/2+\mathbf{p}}^{\dagger} \hat{a}_{\mathbf{q}/2-\mathbf{p}}^{\dagger} + \text{H.c.}). \quad (8)$$

Here \hat{a}^{\dagger} and \hat{a} are creation and annihilation operators of a (spinless) fermion with mass m , while the bare spin 1 bosonic diatomic molecule is created and annihilated by \hat{b}_{μ}^{\dagger} and \hat{b}_{μ} . The vector index μ represents the projection of spin on some axis.

The superfluid described by the Hamiltonian (8) depends on four parameters. Of these, ϵ_0 is the bare detuning, controlling the position of the Feshbach resonance, while the particle number N is the expectation value of the operator

$$\hat{N} = \sum_{\mathbf{p}} \hat{a}_{\mathbf{p}}^\dagger \hat{a}_{\mathbf{p}} + 2 \sum_{\mu, \mathbf{q}} \hat{b}_{\mu \mathbf{q}}^\dagger \hat{b}_{\mu \mathbf{q}}. \quad (9)$$

Often it is convenient to trade the particle number for the Fermi energy ϵ_F . This is defined as the Fermi energy of a free Fermi gas whose particle number coincides with N above, and is explicitly given by

$$\epsilon_F = \frac{(6\pi^2 N)^{2/3}}{2mV^{2/3}}. \quad (10)$$

Another way to represent the particle number is by the interparticle spacing

$$\ell = \left(\frac{V}{N}\right)^{1/3} = \frac{1}{n^{1/3}}, \quad (11)$$

where n denotes the density of particles $n=N/V$.

The interaction term of the Hamiltonian turns two fermions into a boson and vice versa. It is described by the interaction strength $g(|\mathbf{p}|)$, the momentum dependence of which originates in the fact that the interaction is not pointlike, rather the interaction strength is proportional to the momentum space wave function of the molecule. As such, the interaction needs to be supplemented with a cutoff of order $\Lambda \sim 1/R_e$ where R_e is the physical size of the molecule, or the interaction range as discussed in the Introduction. We will write the interaction strength as

$$g(|\mathbf{p}|) = g\xi(|\mathbf{p}|/\Lambda), \quad (12)$$

where g is the asymptotic value of the interaction strength for small momenta and the dimensionless function ξ describes the quick fall-off of the interaction strength for momenta $|\mathbf{p}| \gg \Lambda$. In this paper, for simplicity we will let

$$\xi(x) = \Theta(1-x) = \begin{cases} 1, & x < 1, \\ 0, & x > 1 \end{cases} \quad (13)$$

with Θ the usual step function. The precise shape of the cutoff function does not affect the conclusions of this paper, see the discussion in Sec. III. The parameters $\epsilon_0, \epsilon_F, g, \Lambda$ completely characterize the p -wave superfluid.

Two important dimensionless combinations can be constructed out of these parameters. One is given by

$$\gamma \sim \frac{m^2 g^2}{\ell}. \quad (14)$$

If this parameter is small, $\gamma \ll 1$, then mean-field theory can safely be employed to analyze the Hamiltonian equation (8). In a typical experiment γ is indeed small, being on the order of $\gamma \sim 1/10$ [6,8]. By analogy with s -wave Feshbach resonances, the case of small γ can be termed that of narrow resonance (while the experimentally irrelevant case of $\gamma \gg 1$ can be termed broad p -wave resonance).

The second parameter

$$c_2 = \frac{m^2 g^2 \Lambda}{3\pi^2} \quad (15)$$

can also be formed. Following Ref. [22] we term the superfluid with large c_2 the case of strong p -wave resonance, and correspondingly the case with small c_2 weak resonance. In current experiments, c_2 is typically large, thus the resonances studied so far were strong [8].

It should be emphasized that under the condition $c_2 \gg 1$, it is possible [8] to trade the two-channel model (8) for the one-channel model

$$H_{1-c} = \sum_{\mathbf{p}} \frac{p^2}{2m} \hat{a}_{\mathbf{p}}^\dagger \hat{a}_{\mathbf{p}} - \sum_{\mathbf{p}, \mathbf{p}', \mathbf{q}, \mu} \frac{g(|\mathbf{p}|)g(|\mathbf{p}'|)}{V\epsilon_0} p_\mu p'_\mu \times \hat{a}_{\mathbf{q}/2+\mathbf{p}}^\dagger \hat{a}_{\mathbf{q}/2-\mathbf{p}}^\dagger \hat{a}_{\mathbf{q}/2-\mathbf{p}'} \hat{a}_{\mathbf{q}/2+\mathbf{p}'}. \quad (16)$$

While c_2 is indeed large in current experiments, we prefer to utilize for our analysis the two-channel Hamiltonian, Eq. (8). Indeed, to analyze (16), one typically needs to employ a Hubbard-Stratonovich transformation to turn it into a form similar to Eq. (8) first, and proceed from there. We find it more straightforward to work directly with Eq. (8).

To further elucidate the meaning of the model, Eq. (8) and its relation to real phenomena, we consider the elastic scattering of two atoms with momenta \mathbf{k} and $-\mathbf{k}$ into momenta \mathbf{k}' and $-\mathbf{k}'$. This scattering proceeds via the p -wave channel and its scattering amplitude is given by [28] [we emphasize that this is a partial scattering amplitude, while the full amplitude is given by the standard expression $3f_1(k)P_1(\cos \theta)$ where θ is the angle between the incoming and outgoing momenta]

$$f_1(k) = \frac{k^2}{-\frac{1}{v} + \frac{k_0}{2}k^2 - ik^3}. \quad (17)$$

Here v is called the scattering volume. In terms of the parameters of Eq. (8) it is given by [8]

$$v^{-1} = -\frac{6\pi\omega_0(1+c_2)}{mg^2}, \quad \omega_0 = \frac{\epsilon_0 - \frac{m\Lambda^3 g^2}{9\pi^2}}{1+c_2}. \quad (18)$$

In an experiment, ϵ_0 (and thus ω_0) is tuned by varying the magnetic field. This induces a change in v , with $1/v$ crossing zero as ϵ_0 is decreased (in this regard, the behavior of the scattering volume v is completely equivalent to the behavior of the scattering length a in an s -wave Feshbach resonant scattering).

The parameter k_0 replaces the ‘‘effective range’’ parameter r_0 of the s -wave resonances and is given by

$$k_0 = -\frac{12\pi}{m^2 g^2}(1+c_2). \quad (19)$$

The poles of the scattering amplitudes describe resonant scattering at positive ω_0 and bound states (molecules) at negative ω_0 . These occur at [neglecting the ik^3 term in the denominator of Eq. (17), small at small ω_0]

$$\frac{k^2}{m} \approx \omega_0. \quad (20)$$

This elucidates the meaning of ω_0 introduced in Eq. (18). One can also remark that the total scattering cross section, for the p -wave scattering, is given by [28]

$$\sigma = 12\pi |f_1(k)|^2. \quad (21)$$

ω_0 , as long as it is positive, can be measured in an experiment by looking at the energy of colliding particles at which the scattering cross section σ has a maximum. At the same time ω_0 , and thus ϵ_0 , is varied by the magnetic field according to

$$\omega_0 \sim \frac{\mu_B(B - B_0)}{1 + c_2}, \quad (22)$$

where B_0 is the magnetic field corresponding to the resonance and μ_B is the effective Bohr magneton. Thus measuring ω_0 and $B - B_0$ simultaneously allows us to determine whether the resonance is weak or strong ($c_2 \ll 1$ or $c_2 \gg 1$). Strong resonances will appear as the ones where the slope of the curve ω_0 vs $\mu_B(B - B_0)$ is small.

The dependence of the scattering volume v on the magnetic field B is given by

$$v = - \frac{mg^2}{6\pi\mu_B(B - B_0)}, \quad (23)$$

reminiscent of the magnetic field dependence of the scattering length in an s -wave Feshbach resonance experiment. We notice that if one tunes the magnetic field B off resonance by the amount such that $\mu_B(B - B_0)$ is equal to the Fermi energy of the gas, then the scattering volume will be much smaller than the cube of the interparticle spacing ℓ^3 if the resonance is narrow ($\gamma \ll 1$), and much larger than the cube of the spacing if the resonance is broad ($\gamma \gg 1$). This justifies the name ‘‘narrow’’ vs ‘‘broad.’’ Indeed, in the case of a broad resonance, a v vs $B - B_0$ graph will appear much broader than in the case of a narrow resonance. Notice the complete equivalence of the parameter γ with its s -wave counterpart [6,8,29–33].

We emphasize that other authors, such as the ones of Ref. [23], prefer to restrict the usage of the term ‘‘broad’’ vs ‘‘narrow’’ for c_2 being large or small. While the concrete terminology is a matter of taste, γ is a parameter which more accurately reflects the notion of ‘‘broad’’ vs ‘‘narrow,’’ as these terms are used in the s -wave resonance context.

B. Analysis of the stability of the 3D p -wave condensate

Here we reproduce the analysis of the stability of the 3D p -wave condensate from Ref. [22]. Suppose, at some negative ω_0 , p -wave molecules form whose binding energy is ω_0 . The radial part of their wave function, at distances much larger than the interaction range $R_e \sim 1/\Lambda$, is given by [18,28]

$$\Psi(r) \sim \frac{e^{-\kappa r}}{r} \left(1 + \frac{1}{\kappa r} \right), \quad (24)$$

where $\kappa = \sqrt{m|\omega_0|}$. At distances much smaller than $1/\kappa$ but still much larger than R_e , $R_e \ll r \ll 1/\kappa$, the wave function can be well approximated by

$$\Psi(r) \sim \frac{1}{r^2}. \quad (25)$$

Since

$$\int_{R_e}^{1/\kappa} r^2 dr |\Psi(r)|^2 \sim \frac{1}{R_e}, \quad (26)$$

the normalization condition of the wave function leads to the normalized expression

$$\Psi(r) = \frac{\sqrt{R_e}}{r^2}, \quad (27)$$

independent of ω_0 . In other words, most of the weight of the wave function is concentrated at distances R_e , or the molecules are small.

Suppose two such molecules collide. It is possible that the collision will lead to one molecule forming a strongly bound state, while the atoms of the other molecule absorb the energy and fly apart. It is also possible that three of the atoms form a strongly bound trimer, while the remaining atom flies away [22,23]. The rate of this process can be estimated as follows. The total rate is given by

$$\Gamma \sim n\sigma_{\text{in}}u, \quad (28)$$

where $n = 1/\ell^3$ is the density of particles, u is their relative velocity, and σ_{in} is the inelastic cross section for this process. In turn, σ_{in} can be estimated as a product of the elastic cross section of two small objects size R_e each, or R_e^2 , times the time they spend in the vicinity of each other, R_e/u , times the rate of the decay. That rate may be difficult to calculate, but it must be of order $1/(mR_e^2)$ by dimensional analysis. Gathering terms we find

$$\Gamma \sim \frac{1}{\ell^3} R_e^2 \frac{R_e}{u} \frac{1}{mR_e^2} u = \frac{1}{m\ell^2} \frac{R_e}{\ell}, \quad (29)$$

which matches Eq. (1) given in the Introduction.

Another simple way to derive Γ proceeds as follows. Any transition amplitude, elastic or inelastic, between some states of two molecules or a molecule and an atom, must go as R_e . This result holds true independently of the details of the interaction potential, and is due to the ultraviolet divergences in the p -wave two-channel model, Eq. (8), as explicitly demonstrated for the molecule-atom scattering in Ref. [22]. The inelastic cross section may then be estimated as [28]

$$\sigma_{\text{in}} \sim R_e^2 \frac{k_f}{k_i}, \quad (30)$$

where $k_f = 1/R_e$ is the final momentum of the particle, and $k_i = mu$, with u the incident velocity. This leads to

$$\Gamma \sim \sigma_{in} n u \sim \frac{1}{m \ell^2} \frac{R_e}{\ell}, \quad (31)$$

which coincides with Eq. (29). This derivation makes it clear that Eq. (29) applies not only to molecule-molecule collisions, but also to molecule-atom collisions. We emphasize that the rate given in Eq. (29) is an estimate, and the precise numerical prefactor depends on the details of the interaction potential.

On the BCS side of the resonance, one could argue that the atoms spend some fraction of their time virtually forming molecules. Those will also undergo atom-molecule relaxation so the decay rate, Eq. (29), applies here as well. One can also consider direct three-body recombination of atoms. Experimental and theoretical studies [9,34] lead to a rate numerically close to the one estimated here for the molecule-molecule and molecule-atom relaxation, at the relevant densities.

Is the decay rate given by Eq. (29) too fast, or sufficiently slow? Obviously it must be slow enough for the condensate to form and equilibrate before it decays. In order to determine whether or not equilibration is possible, we estimate the interaction rate between the atoms in the BCS phase and between the molecules in the BEC phase. This rate corresponds to a time scale which clearly does not exceed the equilibration time. Thus, if this energy scale is larger than the decay rate, there is a chance that the condensate would have time to equilibrate.

In the BCS regime, the molecules have positive energy and if left in vacuum decay into atoms. The molecular decay rate, computed at the Fermi energy, corresponds to the time scale at which atoms interact. This rate can be read off the scattering amplitude Eq. (17). For that, we find the pole of this scattering amplitude, not just the real part as in Eq. (20), but also with its imaginary part. It is given by

$$\frac{k^2}{m} \approx \omega_0 - \frac{i}{6\pi} \frac{m^{5/2} g^2}{1 + c_2} \omega_0^{3/2}. \quad (32)$$

The imaginary part is the decay rate.

We estimate it in case of strong resonances, or $c_2 \gg 1$. Substituting c_2 from its definition, Eq. (15), and choosing ω_0 to be the Fermi energy of the gas, or $\omega_0 \sim 1/(m\ell^2)$, we find the interaction energy

$$E_{3D} \sim \frac{1}{m \ell^2} \frac{R_e}{\ell}. \quad (33)$$

Note that the ratio $g^2/(1+c_2)$ is an increasing function of c_2 . Thus for weak resonances when $c_2 \ll 1$, the interaction energy would be even weaker than the one given by Eq. (33). So the case of the strong resonance corresponds to the strongest possible interactions. This, combined with the fact that the p -wave Feshbach resonances experimentally studied so far appear to be strong, prompts us to concentrate in this paper mostly on strong resonances.

Yet, as we see, this interaction has the same functional form as the decay rate, Eq. (29). Of course, these are estimates of these quantities and perhaps numerical coefficients omitted in Eqs. (33) and (29) conspire to make one larger

than the other. But typically we expect that the decay rate and the interaction energy are of the same order, precluding the formation of the condensate before it decays even in the case of strong resonance.

Another way to estimate the interaction rate is in the BEC regime. With the elastic scattering cross section being R_e^2 , the elastic scattering rate is

$$E_{3D,BEC} \sim R_e^2 n u \sim E_{3D} m u R_e \sim E_{3D} \frac{R_e}{\ell}, \quad (34)$$

since mu is the characteristic momentum of the molecules, which is roughly equal to $1/\ell$. Obviously $R_e/\ell \ll 1$, and thus the interaction rate between the molecules in the BEC regime is even slower than the interaction rate between the atoms in the BCS regime. In particular, it is slower than the decay rate of the molecules, thus making the observation of the 3D BEC p -wave condensate even less likely than its BCS counterpart.

We can compare the estimates derived here with the measured decay constants from Ref. [19] (see their Table I). The decay constant is defined as

$$K = \Gamma/n, \quad (35)$$

and for the estimate, Eq. (29) gives (for once, we explicitly reintroduce the constant \hbar)

$$K = \frac{\hbar R_e}{m} \approx 3 \times 10^{-11} \text{ cm}^3 \text{ s}^{-1}. \quad (36)$$

Here we take $R_e = 50$ a.u and take m to be the mass of ${}^6\text{Li}$. This is very close to the measured atom-molecule decay constant and is one order of magnitude smaller than the measured molecule-molecule decay constant. We do not know why the measured molecule-molecule decay constant is faster by a factor of 10, but note that the derivation presented here ignores the details of the short-range physics and could easily be off by a factor of 10.

We also note that Ref. [19] quotes that the elastic scattering rate between the molecules is faster than the inelastic rate, while the estimates presented here point towards the elastic rate being slower than the inelastic rate. We do not know the reason for this discrepancy.

The conclusion is, the 3D p -wave superfluids decay as fast as they interact and do not have time to form before they decay.

III. p -WAVE SUPERFLUID IN TWO DIMENSIONS

A. Two-channel model

We now consider the case of the 2D p -wave superfluid, governed by the same two-channel model, Eq. (8), but in two-dimensional space. Reducing the space dimensionality changes the dimension of the coupling. In fact, the p -wave two-channel model's upper critical dimension is 2 [35,36]. The coupling constant g is now a dimensionless quantity. The linear divergence which led to the appearance of c_2 in the 3D calculations is now replaced by a logarithmic divergence.

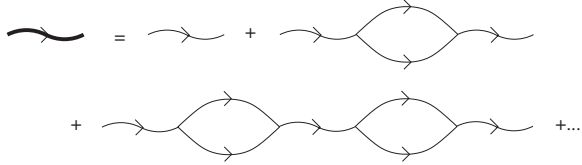


FIG. 1. The renormalized propagator of spin-1 molecules. Here the standard notations for the two-channel model Eq. (9) are used: The thin straight lines are fermionic propagators, the thin wavy lines are bare bosonic propagators, and the thick wavy lines are full bosonic propagators.

As in 3D, it is instructive to compute the scattering amplitude of two atoms. Since to our knowledge this was not done before in the literature for the two-channel model, here we provide its derivation.

According to the Hamiltonian (8) the propagator of fermionic atoms is the free propagator

$$G(p) = \frac{1}{p_0 - p^2/2m + i0}. \quad (37)$$

For simplicity of notation, p is used both as the three-vector (\mathbf{p}, p_0) and as the absolute value of the momentum $|\mathbf{p}|$. The bare propagator of the bosonic spin-1 molecules is equal to

$$D_{\mu\nu}^0(p) = \frac{\delta_{\mu\nu}}{p_0 - p^2/2m - \epsilon_0 + i0} \equiv D^0(p) \delta_{\mu\nu}. \quad (38)$$

The molecular propagator should be renormalized by the presence of fermionic loops as depicted in Fig. 1. The fermionic loop separating molecules of spin μ and ν is diagonal in spin indices and is denoted $\Sigma_{\mu\nu} \equiv \Sigma \delta_{\mu\nu}$. The full propagator is then given by

$$D_{\mu\nu}(p) = \frac{\delta_{\mu\nu}}{D^0(p) - \Sigma(p)} \equiv D(p) \delta_{\mu\nu}, \quad (39)$$

with the fermionic loop taking the value (a factor 2 appears from indistinguishability of the fermions)

$$\begin{aligned} \Sigma_{\mu\nu}(p) &= 2ig^2 \int \frac{d^2q dq_0}{(2\pi)^3} q_\mu q_\nu \xi^2 \left(\frac{|\mathbf{q}|}{\Lambda} \right) G\left(\frac{p}{2} + q\right) G\left(\frac{p}{2} - q\right) \\ &= -\delta_{\mu\nu} \frac{m^2 g^2}{4\pi} \left[\frac{\Lambda^2}{m} + \left(p_0 - \frac{p^2}{4m} \right) \ln \left(1 + \frac{\Lambda^2/m}{\frac{p^2}{4m} - p_0} \right) \right]. \end{aligned} \quad (40)$$

All singularities in the complex p_0 plane lie slightly below the real axis. The molecular propagator becomes

$$D(p) = \frac{1}{p_0 - \frac{p^2}{4m} - \epsilon'_0 + c \left(p_0 - \frac{p^2}{4m} \right) \ln \left(1 + \frac{\Lambda^2/m}{\frac{p^2}{4m} - p_0} \right)}. \quad (41)$$

Here,

$$\epsilon'_0 = \epsilon_0 - \frac{mg^2 \Lambda^2}{4\pi}, \quad (42)$$

is a renormalized detuning, while

$$c = \frac{m^2 g^2}{4\pi} \quad (43)$$

is the constant controlling the strength of the Feshbach resonance, equivalent to c_2 in the 3D calculations.

Just as in 3D, the molecular propagator has a pole at $\mathbf{p} = 0$ and when p_0 is taken to an appropriate value. We denote the real part of the value of p_0 at the pole as ω_0 . The pole corresponds to the binding energy of the molecule if $\omega_0 < 0$ (in which case the pole occurs at $p_0 = \omega_0$) and to the resonance if $\omega_0 > 0$ (in which case only the real part of p_0 is equal to ω_0 at the pole, while the imaginary part of p_0 describes the decay rate of positive binding energy molecules in free space). The value of ω_0 is controlled by tuning ϵ_0 .

We can calculate ω_0 from the condition that it is the real part of p_0 at the pole of the molecular propagator. This gives

$$\epsilon'_0 = \omega_0 + c \omega_0 \ln \left| 1 - \frac{\Lambda^2}{m\omega_0} \right|. \quad (44)$$

Then the (physical) molecular propagator is

$$D(p, p_0 + \omega_0) = \frac{1}{\left(p_0 - \frac{p^2}{4m} \right) \left[1 + c \ln \left(1 + \frac{\Lambda^2/m}{p^2/4m - p_0 - \omega_0} \right) \right] + c \omega_0 \left[\ln \left(1 + \frac{\Lambda^2/m}{p^2/4m - p_0 - \omega_0} \right) - \ln \left| 1 - \frac{\Lambda^2}{m\omega_0} \right| \right]}. \quad (45)$$

Notice that for future convenience we shift the energy p_0 by ω_0 so that p_0 in Eq. (45) measures energy from the binding energy.

Now we can compute the scattering amplitude of two atoms in 2D, just like we did it in 3D in Eq. (18). The elastic scattering of two atoms with incoming momenta \mathbf{k} and $-\mathbf{k}$

into momenta \mathbf{k}' and $-\mathbf{k}'$ proceeds via formation of a molecule, see Fig. 2. Thus the scattering two-atom T -matrix coincides with the propagator $D_{\mu\nu}$ computed at momentum $p=0$, and at energy $p_0 + \omega_0 = k^2/m$, contracted with the incoming momentum k_μ and the outgoing momentum k'_ν . The relationship between the scattering T -matrix and the scatter-

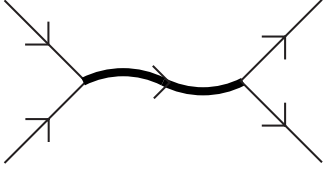


FIG. 2. The diagram corresponding to the scattering of two atoms.

ing amplitude depends on the dimensionality of space. In 2D it is given by (see Appendix A for a derivation)

$$f = -\frac{m}{2\sqrt{2\pi}k}T. \quad (46)$$

This gives for the partial amplitude of p -wave scattering, defined in Eq. (B2),

$$f_1(k) = \left\{ \frac{m\sqrt{k}}{c\sqrt{2\pi}} \left[\frac{\epsilon'_0}{k^2} - \frac{1}{m} \left(c \ln \frac{\Lambda^2}{k^2} + 1 \right) \right] - i\sqrt{\frac{\pi k}{2}} \right\}^{-1}. \quad (47)$$

Here ϵ'_0 can be substituted in terms of ω_0 using Eq. (44), and it is assumed that $\Lambda^2/k^2 \gg 1$. This expression conforms to the general form of the 2D scattering amplitude Eq. (B4). We emphasize that even though it was derived from the 2D version of the two-channel model Eq. (8), only the parameters ϵ'_0 and c follow from that model. Other than that, any p -wave two-dimensional scattering amplitude at low energy must take this form, regardless of the model used (a similar point for the 3D scattering was emphasized in Ref. [8]). This argument will become important in Sec. IV.

The scattering amplitude Eq. (47) has a pole at $k^2/m = \omega_0$ at negative ω_0 and at real part of k^2/m equal to ω_0 at positive ω_0 , just as its 3D counterpart and as follows from the properties of the molecular propagator.

B. Stability of condensates with large molecules

The radial part of the wave function of a 2D p -wave molecule with energy close to zero is given by

$$\Psi(r) \sim \frac{1}{r}. \quad (48)$$

To see this, compare with the 3D case described by Eqs. (24) and (25) and recall that the zero energy solutions of the Schrödinger equation go as $1/r^{l+1}$ in 3D and $1/r^l$ in 2D, where l is the angular momentum. The normalization condition now follows from

$$\int_{R_e}^{1/\kappa} r dr |\Psi(r)|^2 \sim \ln\left(\frac{1}{\kappa R_e}\right), \quad (49)$$

where $\kappa = \sqrt{m|\omega_0|}$, and where, as before, $\omega_0 < 0$ is the binding energy of the molecule. This integral is now divergent logarithmically at both lower and upper limits, so the molecular weight is equally distributed between R_e and $1/\kappa$. Thus, the size of the molecule is no longer R_e , as it was in 3D, but rather $1/\kappa$.

To compute the rate of the atom-molecule relaxation, we go through the same steps as we did in Sec. II B. However, we need to take into account that the molecules no longer have size R_e , but rather $1/\kappa$. Let us do it, for generality reasons, in an arbitrary number of dimensions d .

The decay rate is still given by

$$\Gamma \sim n\sigma_{\text{in}}u, \quad (50)$$

where n is the density, σ_{in} is the inelastic cross section, and u is the velocity, just as in 3D, Eq. (28). However, the meaning of the inelastic scattering cross section σ_{in} is now different. We now have two objects of the size $1/\kappa$ colliding inelastically. The inelastic cross section is given by the product of their elastic cross section, proportional to $1/\kappa^{d-1}$, the time the molecules spent together, given by $1/(\kappa u)$, and the collapse rate during that time, $1/(mR_e^2)$. This should still be multiplied by the probability that the three atoms out of four which constitute two molecules find themselves at distance R_e from each other, so that they were all at distances of the order of the force range between them. To find this probability is not a simple problem. We have three fermions, each pair interacting strongly since they are close to a p -wave Feshbach resonance.

Suppose their three-body wave function is given by the following scaling ansatz:

$$\psi(r) \sim r^\gamma. \quad (51)$$

Here r denotes a collective coordinate of the three particles, such as, for example, a hyperspherical radius. Equation (52) serves as a definition of a scaling exponent γ . Then, the probability that three fermions find themselves at a distance R_e from each other is given by

$$P \sim (R_e\kappa)^{2d+2\gamma}. \quad (52)$$

The power of $2d$ comes about because of the phase volume of setting two fermions at a distance R_e from the third one, while 2γ arises from the behavior of the square of the wave function, $|\psi|^2 \sim r^{2\gamma}$. Setting all these factors together gives

$$\Gamma \sim n \left(\frac{1}{\kappa}\right)^{d-1} \frac{1}{mR_e^2} \frac{1}{\kappa u} (R_e\kappa)^{2d+2\gamma} u = \frac{1}{m\ell^d \kappa^{d-2}} (R_e\kappa)^{2d+2\gamma-2}. \quad (53)$$

Finally, close to Feshbach resonance, the size of the molecules is close to their separation, or $1/\kappa \sim \ell$. Then Eq. (53) simplifies to give

$$\Gamma \sim \frac{1}{m\ell^2} \left(\frac{R_e}{\ell}\right)^{2d+2\gamma-2}. \quad (54)$$

This is the final answer for the decay rate of large molecules.

Let us check that this expression indeed gives the correct answer in the case of 3D s -wave molecules (which are large). In this case, $d=3$, and $\gamma \approx -0.22$ [20,21]. Then

$$\Gamma \sim \frac{1}{m\ell^2} \left(\frac{R_e}{\ell}\right)^{3.55}, \quad (55)$$

as was indeed derived in Ref. [20], and as was discussed in the Introduction, Eq. (2). For easier comparison with Ref.

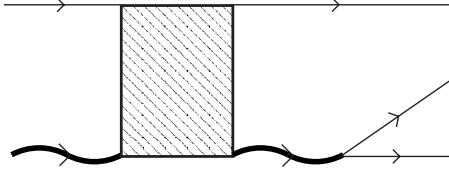


FIG. 3. The diagram corresponding to the wave function of free fermions. The square block represents the atom-molecule T -matrix, and the three outgoing fermionic lines represent the three fermions whose wave function we would like to compute.

[20], recall that it is sometimes beneficial to introduce the decay constant $K = \Gamma/n$ as in Eq. (35). Recall also that in the 3D s -wave problem, $\kappa = 1/a$, where a is the scattering length. This gives

$$K \sim \frac{R_e}{m} \left(\frac{R_e}{a} \right)^{2.55}, \quad (56)$$

the form discussed in Ref. [20].

We also briefly examine the case of 3D s -wave bosons close to Feshbach resonance. Then $\gamma = -2$ (as a consequence of the presence of Efimov states) and Eq. (54) gives

$$\Gamma \sim \frac{1}{m\ell^2}. \quad (57)$$

A decay constant for the boson problem is defined as $K = \Gamma/n^2$. Substituting the scattering length a for ℓ we find

$$K \sim \frac{a^4}{m}, \quad (58)$$

a well-known form for the boson problem [37–40].

When applied to the 2D p -wave problem, Eq. (54) gives

$$\Gamma \sim \frac{1}{m\ell^2} \left(\frac{R_e}{\ell} \right)^{2+2\gamma}. \quad (59)$$

At issue now is calculating the exponent γ . This calculation is the subject of the next two sections.

C. Three-body problem

We need to compute the three-body wave function close to Feshbach resonance. This can be done in either coordinate or momentum space. We are going to present the momentum space derivation, since it can be done using the standard techniques of many-body theory.

First, let us show that the scaling of the three-body wave function is related to the behavior of the three-body scattering amplitude. Suppose a three-body scattering matrix T , depicted in Fig. 3, is known. It is a function of the incoming momenta and energy, and the outgoing momenta and energy. To arrive at the wave function of three particles, we fix the incoming momenta and energy to be on shell. Then we multiply the T matrix by the four outgoing Green’s functions, one bosonic and three fermionic. Finally we Fourier transform with respect to the fermionic outgoing momenta, respecting the momentum-energy conservation. For the illus-

tration of this procedure, see Eq. (A1) which represents this in case of just one particle scattering off a potential.

Suppose the T -matrix scales as p^γ , where p represents the overall momentum scale. Then it is easy to figure out the scaling of the wave function. There are three outgoing energies and momenta, corresponding to the three outgoing fermionic lines. However, the energy-momentum conservation restricts the number of linear independent energies and momenta to two. Hence there are two integrals over energy and momentum, contributing the power $2(d+2)$ (energy is counted as momentum squared). There are four outgoing propagators, one bosonic Eq. (45) and three fermionic Eq. (37), contributing the power -8 (the bosonic propagator includes logarithms, but these are irrelevant for the purpose of power counting). Finally there is a vertex where a bosonic line splits into two fermions, contributing a power 1 due to the p -wave momentum-dependent factor. Taking all of these factors into account, and remembering that the coordinate scaling is opposite in sign to the momentum scaling, we find that the scaling of the wave function is given by

$$\gamma = -[\gamma' + 2(d+2) - 8 + 1], \quad (60)$$

or in two dimensions,

$$\gamma = -\gamma' - 1. \quad (61)$$

To proceed, we need to know the scaling of the T -matrix, representing the scattering of a fermion and a spin-1 molecule.

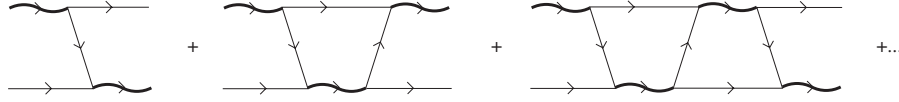
D. Solution of the three-body problem

In the scattering problem, let the incoming molecule have spin μ and the outgoing spin ν . The T -matrix will then in general be a tensor $T_{\mu\nu}$. In the center-of-mass frame, with the incoming molecule having momentum \mathbf{k} and the outgoing \mathbf{p} , the tensor $T_{\mu\nu}$ consists of five terms proportional to $\delta_{\mu\nu}$, $p_\mu p_\nu$, $p_\mu k_\nu$, $k_\mu p_\nu$, and $k_\mu k_\nu$. However, we are interested in the wave function at short range $r \ll 1/\kappa$, which corresponds to large p , or $p \gg k \sim \kappa$. Then it is sufficient to set $\mathbf{k} = 0$. Thus we write [24]

$$\begin{aligned} T_{\mu\nu}(\mathbf{p}, p_0) &\equiv T_1(p, p_0)\delta_{\mu\nu} + T_2(p, p_0)p_\mu p_\nu / p^2 \\ &\equiv \sum_{i=1,2} T_i(p, p_0)u_{\mu\nu}^i(\mathbf{p}), \end{aligned} \quad (62)$$

which defines the set of basis tensors $\{u_{\mu\nu}^{1,2}(\mathbf{p})\} = \{\delta_{\mu\nu}, p_\mu p_\nu / p^2\}$.

The scattering T -matrix is the sum of the series of diagrams indicated in Fig. 4. These diagrams appear the same as those studied in the s -wave three-body problem [41,42], however the Feynman rules are of course different in the present problem. For weak resonances, the diagrams form a perturbative series in which only the first few diagrams may be kept. However, for the strong resonances studied in the present paper the diagrams are all of the same order and the sum of the series of diagrams is needed. The summation may be attained by constructing a Lippmann-Schwinger-type integral equation for the scattering amplitude. This summation was performed in a similar manner in the three-dimensional

FIG. 4. The series of diagrams which sum to give the scattering T -matrix of a spin-1 molecule and a fermionic atom.

problem studied in Ref. [22] (see also Ref. [23]). The kinematics are chosen as follows: The incoming molecule is on-shell with three-momentum $(\mathbf{0}, \omega_0)$ while the incoming atom has three-momentum $(\mathbf{0}, 0)$. The outgoing molecule has $(\mathbf{p}, p_0 + \omega_0)$ and the outgoing fermion $(-\mathbf{p}, -p_0)$. The scattering matrix does not include external lines. Then the integral equation takes the form

$$\begin{aligned}
 T_{\mu\nu}(\mathbf{p}, p_0) = & -2Zg(p)g(p/2)G(p, p_0 + \omega_0)p_\mu p_\nu \\
 & -4i \int \frac{d^2q dq_0}{(2\pi)^3} T_{\mu\alpha}(\mathbf{q}, q_0)G(q, -q_0) \\
 & \times G(\mathbf{p} + \mathbf{q}, p_0 + q_0 + \omega_0)D(q, q_0 + \omega_0) \\
 & \times \left(p + \frac{q}{2} \right)_\alpha \left(q + \frac{p}{2} \right)_\nu g\left(\left| \mathbf{p} + \frac{\mathbf{q}}{2} \right| \right) g\left(\left| \mathbf{q} + \frac{\mathbf{p}}{2} \right| \right). \quad (63)
 \end{aligned}$$

Repeated indices are summed over. Z is the residue of the molecular propagator at the pole and is needed for correct normalization of the scattering matrix. It is a function of ω_0 and c whose precise value will not be needed in the following.

The integral over q_0 in Eq. (63) may be performed by closing the contour in the upper half-plane, setting $q_0 \rightarrow -q^2/2m$. In order to solve the integral equation it is then convenient to let $p_0 \rightarrow -p^2/2m$. This ensures that the frequency dependence of $T_{\mu\nu}$ is the same on both sides of the integral equation. The integral equation is then solved for $T_i(p) \equiv T_i(p, -p^2/2m)$. Subsequently, this solution can then be used to find $T_i(p, p_0)$ at any $p_0 \leq 0$.

To project onto the functions T_1 and T_2 defined in Eq. (62) multiply the integral equation (63) by $u_{\mu\nu}^k(\mathbf{p})$. The left-hand side will then contain the matrix

$$U_{ki} = u_{\mu\nu}^k(\mathbf{p})u_{\mu\nu}^i(\mathbf{p}) = \begin{pmatrix} 2 & 1 \\ 1 & 1 \end{pmatrix}_{ki}. \quad (64)$$

This matrix is invertible and it is thus possible to find a set of coupled integral equations for the functions $T_1(p)$ and $T_2(p)$. Upon multiplying Eq. (63) by $U_{jk}^{-1}u_{\mu\nu}^k(\mathbf{p})$ it becomes

$$\begin{aligned}
 T_j(p) = & -2Zg(|\mathbf{p}|)g(|\mathbf{p}|/2)G(p, -p^2/2m + \omega_0)p^2\delta_{2j} \\
 & - \frac{mg^2}{\pi^2} \int qdqD(q, -q^2/2m + \omega_0)b_{ji}(p, q)T_i(q, \\
 & -q^2/2m). \quad (65)
 \end{aligned}$$

The dimensionless matrix b is given by

$$\begin{aligned}
 b_{ji}(p, q) \equiv & \frac{1}{m}U_{jk}^{-1} \int_0^{2\pi} d\theta \frac{\xi(|\mathbf{p} + \mathbf{q}/2|/\Lambda)\xi(|\mathbf{q} + \mathbf{p}/2|/\Lambda)}{\omega_0 - p^2/m - q^2/2 - \mathbf{p} \cdot \mathbf{q}/m} \\
 & \times u_{\mu\nu}^k(\mathbf{p})u_{\mu\alpha}^i(\mathbf{q})(p + q/2)_\alpha(q + p/2)_\nu, \quad (66)
 \end{aligned}$$

with θ the angle between \mathbf{p} and \mathbf{q} .

To further simplify, assume that both p and q are cut off at Λ using the usual step function. Then the matrix b may be calculated with the result

$$b_{11} = \frac{\pi}{p^2} [\sqrt{(\omega - p^2 - q^2)^2 - p^2q^2} + \omega - p^2 - q^2], \quad (67)$$

$$\begin{aligned}
 b_{12} = & -\pi + \pi \frac{(2\omega - 2p^2 - q^2)(\omega - p^2 - q^2)}{p^2q^2} \\
 & + \frac{\pi}{\sqrt{(\omega - p^2 - q^2)^2 - p^2q^2}} \\
 & \times \left(\frac{(2\omega - 2p^2 - q^2)(\omega - p^2 - q^2)^2}{p^2q^2} - 2\omega + 2p^2 + q^2 \right), \quad (68)
 \end{aligned}$$

$$\begin{aligned}
 b_{21} = & -\frac{5\pi}{2} + \frac{\pi}{2} \frac{3p^2 + 3q^2 - 5\omega}{\sqrt{(\omega - p^2 - q^2)^2 - p^2q^2}} \\
 & - \frac{2\pi}{p^2} [\sqrt{(\omega - p^2 - q^2)^2 - p^2q^2} + \omega - p^2 - q^2], \quad (69)
 \end{aligned}$$

$$\begin{aligned}
 b_{22} = & -\frac{\pi}{2} - \pi \frac{(4\omega - 3p^2 - 2q^2)(\omega - p^2 - q^2)}{p^2q^2} \\
 & + \frac{\pi/2}{\sqrt{(\omega - p^2 - q^2)^2 - p^2q^2}} \\
 & \times \left(-2 \frac{(4\omega - 3p^2 - 2q^2)(\omega - p^2 - q^2)^2}{p^2q^2} \right. \\
 & \left. + 3\omega - 3p^2 - q^2 \right). \quad (70)
 \end{aligned}$$

Here a dimensionless detuning is defined as $\omega \equiv \omega_0 \frac{m}{\Lambda^2}$.

According to Eq. (51), in order to determine the behavior of the three-body wave function, the functions $T_1(p)$ and $T_2(p)$ are needed for momenta $\sqrt{-m\omega_0} \ll p \leq \Lambda$. We now proceed to solve Eq. (65) analytically in this range of momenta. In the following, the limit $c \rightarrow \infty$ will be taken to ensure that the Feshbach resonances studied are strong. For momenta in the range of interest the integral equation reduces to

$$T_j(p) = 2Zg^2m\delta_{2,j} + \frac{8}{3\pi} \int_{\kappa}^{\Lambda} \frac{dq}{q} \frac{b_{ji}(p/q)}{\ln\left(\frac{\Lambda}{q}\right)} T_i(q). \quad (71)$$

The matrix b takes the limiting forms

$$\kappa \ll p \ll q \ll \Lambda: b = \begin{pmatrix} -\frac{\pi}{2} + \frac{3\pi p^2}{8q^2} & -\frac{\pi}{2} + \frac{5\pi p^2}{8q^2} \\ -\frac{9\pi p^4}{16q^4} & -\frac{3\pi p^4}{16q^4} \end{pmatrix}, \quad (72)$$

$$\kappa \ll q \ll p \ll \Lambda: b = \begin{pmatrix} -\frac{\pi q^2}{2p^2} & -\frac{\pi q^2}{4p^2} \\ -\pi + \frac{7\pi q^2}{4p^2} & -\frac{\pi}{2} + \frac{7\pi q^2}{8p^2} \end{pmatrix}. \quad (73)$$

Equation (71) suggests a solution of the form

$$T_1(p) = C_1 \ln^{\alpha}\left(\frac{\Lambda}{p}\right), \quad T_2(p) = C_2 \ln^{\alpha}\left(\frac{\Lambda}{p}\right). \quad (74)$$

Substituting into Eq. (71) and keeping leading terms results in the set of linear equations for the coefficients C_1 and C_2 ,

$$\begin{aligned} C_1 \ln^{\alpha}\left(\frac{\Lambda}{p}\right) &= -\frac{4}{3\alpha} \left[C_1 \ln^{\alpha}\left(\frac{\Lambda}{p}\right) + C_2 \ln^{\alpha}\left(\frac{\Lambda}{p}\right) \right], \\ C_2 \ln^{\alpha}\left(\frac{\Lambda}{p}\right) &= -\frac{4}{3\alpha} \left\{ 2C_1 \left[\ln^{\alpha}\left(\frac{\Lambda}{\kappa}\right) - \ln^{\alpha}\left(\frac{\Lambda}{p}\right) \right] \right. \\ &\quad \left. + C_2 \left[\ln^{\alpha}\left(\frac{\Lambda}{\kappa}\right) - \ln^{\alpha}\left(\frac{\Lambda}{p}\right) \right] \right\} + 2Zg^2m. \end{aligned} \quad (75)$$

This set of equations has solutions only if $\alpha = \pm \frac{4}{3}i$. Matching coefficients finally results in the solutions

$$\begin{aligned} T_1(p) &= \rho \cos \left[\frac{4}{3} \ln \ln \left(\frac{\Lambda}{p} \right) + \phi + \frac{3\pi}{4} \right], \\ T_2(p) &= \sqrt{2}\rho \cos \left[\frac{4}{3} \ln \ln \left(\frac{\Lambda}{p} \right) + \phi \right], \end{aligned} \quad (76)$$

with the amplitude satisfying

$$\rho = \frac{\sqrt{2}Zg^2m}{\cos \left[\frac{4}{3} \ln \ln (\Lambda/\kappa) \right]}. \quad (77)$$

This solution contains a free parameter, as it does not allow for the determination of both ρ and ϕ independently.

In solving Eq. (65) numerically, it is found that the overall amplitude of the solutions $T_1(p)$ and $T_2(p)$ converges very slowly. We attribute this slow convergence to the logarithmic behavior of the solutions; in the numerical study it is important to keep $\ln(\Lambda/\kappa) \gg 1$ while simultaneously the configu-

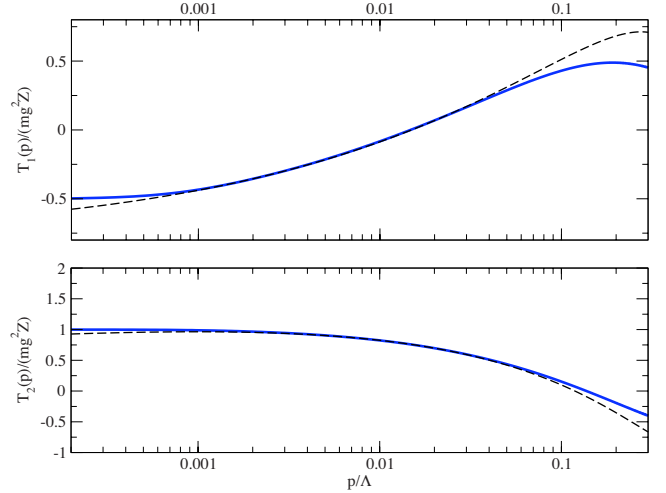


FIG. 5. (Color online) $T_1(p)$ and $T_2(p)$ obtained by solving Eq. (65) for $\omega_0 = -10^{-6} \frac{\Lambda^2}{m}$ and $c_2 = 10^6$ (blue, solid). The solution uses Gaussian-Legendre quadrature for the numerical integration [43] with 2000 grid points. Also shown are the analytical solutions (78) with parameters chosen as in Eq. (79) (black, dashed).

ration space must contain a large number of momenta p for which $\ln(\kappa/p) \gg 1$. Having this in mind, we therefore write the solutions as

$$T_i(p) = \rho_i \cos \left[\frac{4}{3} \ln \ln \left(\frac{\Lambda}{p} \right) + \phi_i \right], \quad i = 1, 2 \quad (78)$$

and determine the ratio ρ_2/ρ_1 rather than the separate values of these amplitudes.

The solutions $T_1(p)$ and $T_2(p)$ of the coupled integral equations (65) are shown in Fig. 5 for a large value of c_2 . Also shown are the analytical solutions (78) with the parameters

$$\begin{aligned} \phi_1 &= 2.80, & \phi_2 &= 0.56, \\ \rho_1 &= 0.71 & \rho_2 &= 0.96. \end{aligned} \quad (79)$$

We observe that $\phi_1 - \phi_2 \approx 3\pi/4$ and $\rho_2/\rho_1 \approx \sqrt{2}$, both with a 5% error. Thus we conclude that the analytical expressions given in Eq. (76) are correct.

E. Lifetime and the interaction energy of the 2D p -wave condensates

We are now in a position to finish the calculation of the lifetime of the 2D p -wave condensate. The scattering amplitude is given by Eq. (62), where in turn T_1 and T_2 are given by Eq. (76). These expressions do not scale at all, corresponding to $\gamma' = 0$. Thus, according to Eq. (61),

$$\gamma = -\gamma' - 1 = -1. \quad (80)$$

Substituting this into Eq. (59) we find

$$\Gamma \sim \frac{1}{m\ell^2}, \quad (81)$$

which gives the decay rate of the 2D p -wave superfluid as discussed in the Introduction, in Eq. (3).

This should be compared with the interaction rate for the 2D p -wave atoms at the Fermi energy of the gas. We find this energy first in the BCS regime by examining the scattering amplitude of two atoms at positive ω_0 , as found earlier in Eq. (47). The imaginary part of the pole of this scattering amplitude, computed at $\omega_0 = \epsilon_F$, gives us the needed interaction rate, quite analogously with Eq. (32) which we employed in 3D. The answer crucially depends on whether the parameter

$$c \ln\left(\frac{\ell}{R_e}\right) \quad (82)$$

is large or small (as before, ℓ is the interparticle separation and $R_e = 1/\Lambda$ is the interaction length scale). As in the 3D case, we can term the case when this parameter is large as strong resonance, although unlike in 3D, any resonance when the gas is sufficiently dilute becomes strong. If the resonance is weak, then $c \ll 1$, since the logarithm in Eq. (82) is always large.

Assuming that the resonance is strong, we find the pole of Eq. (47) to be at

$$\frac{k^2}{m} \approx \omega_0 - i \frac{\pi \omega_0}{\ln\left(\frac{\Lambda^2}{m \omega_0}\right)}. \quad (83)$$

In the opposite case of weak resonance, we find

$$\frac{k^2}{m} \approx \omega_0 - i \pi c \omega_0. \quad (84)$$

Substituting $\omega_0 = \epsilon_F$, we estimate from here the atomic interaction energy as

$$E_{2D} \sim \frac{1}{m \ell^2} \frac{1}{\ln\left(\frac{\ell}{R_e}\right)} \quad (85)$$

in the case when the resonance is strong and

$$E_{2D} \sim \frac{c}{m \ell^2} \quad (86)$$

when the resonance is weak. We expect that in a typical experiment the gas will be dilute so the resonance will be strong, which is why we quoted Eq. (85) in the Introduction, Eq. (6). In either of these two cases, we see that the interaction energy is much smaller than the decay rate, given by Eq. (81), so we expect purely 2D p -wave gases to be unstable.

Likewise, in the BEC regime, we need to estimate the elastic scattering rate of two molecules. The molecules (unlike atoms) scatter in the s -wave channel. The scattering of two molecules in 2D must proceed according to the standard rules of quantum mechanics, which predicts that the s -wave scattering cross section of particles at sufficiently low momentum k goes as [28]

$$\sigma_{el} = \frac{\pi^2}{k} \frac{1}{\ln^2\left(\frac{\alpha}{k R_e}\right) + \frac{\pi^2}{4}}, \quad (87)$$

where the unknown constant α depends on the details of the interactions. This gives for the elastic collision rate (taking k of the order of $1/\ell$)

$$E_{2D, \text{BEC}} = \sigma_{el} \mu u \sim \frac{\pi^2}{m \ell^2} \frac{1}{\ln^2\left(\frac{\ell}{\alpha R_e}\right) + \frac{\pi^2}{4}}. \quad (88)$$

This energy is somewhat smaller than the BCS estimate, Eq. (85), but since the logarithmic factor is not very large, we can think of it as being of the same order as Eq. (85). Thus the BEC 2D superfluid is as unstable as its BCS counterpart.

IV. QUASI-2D SUPERFLUID

Now let us consider the last remaining question, the stability of a 2D p -wave superfluid confined to a pancake of width d . Such a superfluid is still described by Eq. (8), but with the additional presence of a confining potential in the third direction, which we denote z ,

$$V(z) = \frac{1}{2} m \omega_z^2 z^2, \quad (89)$$

where ω_z is the confining frequency. The width of the pancake d is related to the oscillator frequency via

$$d \sim \frac{1}{\sqrt{m \omega_z}}. \quad (90)$$

The quasi-2D regime is

$$R_e \ll d \ll \ell. \quad (91)$$

$R_e \ll d$ because otherwise the physics of the Feshbach resonance is modified by the confinement (also, R_e is very short so that the confinement to the scale below R_e is not currently technologically possible), while $d \ll \ell$ in order for the gas to be truly confined to 2D.

The scattering of identical fermions close to a p -wave Feshbach resonance follows from this Hamiltonian. Calculating it in the confined geometry is an involved problem, first solved for the case of s -wave resonance confined to 2D in Refs. [44,45] (see also the first calculation of this type, done for the s -wave gas confined to 1D, in Ref. [46]). For the case of p -wave resonances, this problem was studied in Ref. [47] in both 1D and 2D. Yet, for our purposes, we do not need to know the answer. It is enough to know that the scattering is still described by Eq. (47), albeit with coefficients c and ϵ'_0 no longer related to the parameters of the Hamiltonian equation (8) the way they were before, but rather being some more complicated functions, which also depend on d among other parameters. This is because any low-energy p -wave scattering in two dimensions must be described by the expression (B4), with the function $g_1(k)$ having the low k expansion as in Eq. (47).

Thus the interaction energy of the two atoms confined to this geometry, derived in the preceding section by using Eq.

(47) only, is still given by Eq. (85) or Eq. (86). The only difference is that R_e in these relations should be traded for d , as d is now the smallest length scale at which the 2D physics is still at work.

Yet the interaction rate of the molecules in the BEC regime will actually be given by the 3D formula (34). This is related to the fact that in a quasi-2D geometry, the coefficient α in Eq. (88) is typically anomalously large, and leads to [45]

$$E_{\text{quasi-2D,BEC}} \sim \frac{1}{m\ell^2} \frac{R_e^2}{d^2}. \quad (92)$$

This energy scale is very small, thus there is no hope to observe the BEC of p -wave molecules, even in the quasi-2D geometry. So we concentrate on the case of the BCS phase.

Now the decay rate in quasi-2D can be deduced in the following way. Atoms decay when three of them approach each other at distance R_e . This distance is much shorter than d , so that the 3D decay physics must take over. So we should not use Eq. (81) to compute the decay rate. Rather, we need to revert back to the appropriate expression in 3D, given by Eq. (29), with one modification. In Eq. (29), ℓ denotes average distance between the particles in three dimensions, while Eq. (85) and Eq. (86) are written in terms of average distance between particles in two dimensions. These are related by the obvious

$$\ell_{3D}^3 = \ell_{2D}^2 d. \quad (93)$$

This leads to the decay rate

$$\Gamma_{\text{quasi-2D}} \sim \frac{1}{m\ell^2} \frac{R_e}{d}, \quad (94)$$

where ℓ is now the two-dimensional distance. This concludes the derivation of Eq. (4).

We therefore see that the necessary condition for the existence of a stable superfluid in the quasi-2D geometry is given by $E_{2D} \gg \Gamma_{\text{quasi-2D}}$ or

$$\max \left[\ln \left(\frac{\ell}{d} \right), \frac{1}{c} \right] \ll \frac{d}{R_e}. \quad (95)$$

Since logarithms, even of large arguments, are typically not very large (we assume c is a constant generally of the order of 1, although its value is controlled purely by a particular Feshbach resonance and it can be calculated from its physics on a case by case basis), it is possible that this condition will be satisfied in experiments.

Indeed, a typical value for d would be, perhaps, one-half a wavelength of the light used to create a confining potential. This gives $d \sim 250$ nm, or 5×10^3 a.u. With $\ell \sim 10^4$ a.u., the ratio $\ell/d \sim 2$, and its logarithm is basically 1. At the same time d/R_e can be kept just marginally smaller than 200. So Eq. (95) is satisfied with a large margin.

Yet we must remember that Eq. (95) is but a necessary condition for the decay being slow enough to allow for equilibration of the superfluid. In practice, the equilibration involves many collisions between atoms and may go much slower than E_{2D} . In truth we have only one example of a decay slow enough that we know from experiment that there

is sufficient time for equilibration and meaningful experiments in the superfluid phase, that of the 3D s -wave case. In that case, the ratio of the Fermi energy (as a crude estimate of the characteristic energy of the condensate) to the decay rate is an impressive $(\ell/R_e)^{3.55} \sim 10^8$. The p -wave superfluids confined to 2D are far from being that stable.

V. CONCLUSIONS

This concludes our studies of the stability of the fermionic paired superfluids close to p -wave Feshbach resonance. From the analysis of this paper, it is clear that the 3D p -wave gases are inherently unstable. The situation improves if they are confined to 2D. Yet it is nowhere near the case of 3D s -wave superfluids, which are stable for all practical purposes due to a very high scaling power in their decay rate, Eq. (55). A promising route to increase stability further in a quasi-2D setting seems to be a creative application of the optical lattice, similar to what was recently done in Ref. [48] for a different problem. This should be a subject of further work.

ACKNOWLEDGMENTS

We acknowledge support by NSF via Grant No. DMR-0449521 (V.G. and J.L.), by EPSRC Grant No. GR/S61263/01 (N.C.), and by the IFRAF Institute and ANR Grant No. 06-NANO-014 (J.L.). We thank D. Petrov for useful discussions and C. H. Greene for helpful remarks.

APPENDIX A: RELATIONSHIP BETWEEN THE T-MATRIX AND THE SCATTERING AMPLITUDE IN 2D

Consider a particle of mass m scattering in a potential in 2D. Its wave function is given by

$$\psi(\mathbf{r}) = e^{i\mathbf{k}\mathbf{r}} + \int \frac{d^2p}{(2\pi)^2} \frac{1}{E - \frac{p^2}{2m} + i0} T(\mathbf{k}, \mathbf{p}) e^{i\mathbf{p}\mathbf{r}}, \quad (A1)$$

where $T(\mathbf{k}, \mathbf{p})$ is the scattering T -matrix computed between momenta \mathbf{k} and \mathbf{p} at energy $E = k^2/(2m)$. We compare this expression with the definition of the scattering amplitude in 2D, given by the large r expression of the wave function [28]

$$\psi(\mathbf{r}) = e^{i\mathbf{k}\mathbf{r}} + f(k, \varphi) \frac{e^{ikr}}{\sqrt{-ir}}, \quad \sqrt{-i} = \exp(-i\pi/4), \quad (A2)$$

where φ is the angle between the incoming momentum \mathbf{k} and the position vector \mathbf{r} . Doing the angular part of the integral in Eq. (A1) at large r by the steepest descent method we find

$$\begin{aligned} \psi(\mathbf{r}) &= e^{i\mathbf{k}\mathbf{r}} + \int_0^\infty \frac{pdp}{4\pi^2} \\ &\times \left(T(\mathbf{k}, \mathbf{p}_r) \sqrt{\frac{2\pi}{ipr}} e^{ipr} + T(\mathbf{k}, -\mathbf{p}_r) \sqrt{\frac{2\pi}{-ipr}} e^{-ipr} \right) \\ &\times \frac{1}{\frac{k^2}{2m} - \frac{p^2}{2m} + i0}, \end{aligned} \quad (A3)$$

where \mathbf{p}_r denotes a vector whose length is p , but which is directed along \mathbf{r} . Change variables in the second integral to get

$$\int_{-\infty}^{\infty} \frac{p dp}{4\pi^2} T(\mathbf{k}, \mathbf{p}_r) \sqrt{\frac{2\pi}{ipr}} e^{ipr} \frac{1}{\frac{k^2}{2m} - \frac{p^2}{2m} + i0}, \quad (\text{A4})$$

where the contour of integration goes above the $p=0$ singularity. Performing the integral by residues gives

$$\psi(\mathbf{r}) = e^{i\mathbf{k}\mathbf{r}} - \frac{mi}{\sqrt{2\pi ikr}} T(\mathbf{k}, \mathbf{k}_r) e^{ikr}. \quad (\text{A5})$$

Comparing with Eq. (A2) gives

$$f = -\frac{m}{\sqrt{2\pi k}} T(\mathbf{k}, \mathbf{k}'). \quad (\text{A6})$$

When comparing this expression with the one used in the text, Eq. (46), one needs to remember that m in Eq. (A6) is the reduced mass of two fermions and should be replaced according to $m \rightarrow m/2$.

APPENDIX B: CONSTRAINTS PLACED ON THE SCATTERING AMPLITUDE IN 2D BY UNITARITY

The scattering amplitude in 2D is constrained by unitarity, just like its 3D counterpart. Here we reproduce the appropriate derivation from Ref. [28].

Consider the scattering of a particle of mass m with momentum \mathbf{k} into the momentum \mathbf{k}' such that $k=k'$, but the angle between these two vectors is φ . The scattering amplitude can be expressed in terms of the phase shifts δ_l according to [28]

$$f(k, \varphi) = \frac{1}{i\sqrt{2\pi k}} \sum_{l=-\infty}^{\infty} (e^{2i\delta_l} - 1) e^{il\varphi}. \quad (\text{B1})$$

Introduce the partial scattering amplitudes

$$f_l(k) = \frac{1}{i\sqrt{2\pi k}} (e^{2i\delta_l} - 1). \quad (\text{B2})$$

Since

$$|e^{2i\delta_l}|^2 = 1, \quad (\text{B3})$$

a constraint on the form $f_l(k)$ can be as follows:

$$f_l(k) = \frac{1}{g_l(k) - i\sqrt{\frac{\pi k}{2}}}. \quad (\text{B4})$$

Here $g_l(k)$ are *real* functions of k .

Thus only the functions $g_l(k)$ remain undetermined in an arbitrary scattering process. Yet their low k expansions take a universal form, up to the coefficients of the expansion [28]. It is these coefficients which need to be calculated on a case by case basis [see Eq. (47) for the low k expansion of $g_1(k) = g_{-1}(k)$].

-
- [1] C. A. Regal, M. Greiner, and D. S. Jin, Phys. Rev. Lett. **92**, 040403 (2004).
[2] M. W. Zwierlein, C. A. Stan, C. H. Schunck, S. M. F. Raupach, A. J. Kerman, and W. Ketterle, Phys. Rev. Lett. **92**, 120403 (2004).
[3] G. B. Partridge, K. E. Strecker, R. I. Kamar, M. W. Jack, and R. G. Hulet, Phys. Rev. Lett. **95**, 020404 (2005).
[4] S. S. Botelho and C. A. R. Sá de Melo, J. Low Temp. Phys. **140**, 409 (2005).
[5] T.-L. Ho and R. B. Diener, Phys. Rev. Lett. **94**, 090402 (2005).
[6] V. Gurarie, L. Radzihovsky, and A. V. Andreev, Phys. Rev. Lett. **94**, 230403 (2005).
[7] C.-H. Cheng and S.-K. Yip, Phys. Rev. Lett. **95**, 070404 (2005).
[8] V. Gurarie and L. Radzihovsky, Ann. Phys. **322**, 2 (2007).
[9] C. A. Regal, C. Ticknor, J. L. Bohn, and D. S. Jin, Phys. Rev. Lett. **90**, 053201 (2003).
[10] C. Ticknor, C. A. Regal, D. S. Jin, and J. L. Bohn, Phys. Rev. A **69**, 042712 (2004).
[11] D. Vollhardt and P. Wolfe, *The Superfluid Phases Of Helium 3* (Taylor and Francis, New York, 2002).
[12] G. E. Volovik, *Exotic Properties of Superfluid ^3He* (World Scientific, Singapore, 1992).
[13] N. Read and D. Green, Phys. Rev. B **61**, 10267 (2000).
[14] D. A. Ivanov, Phys. Rev. Lett. **86**, 268 (2001).
[15] A. Yu. Kitaev, Ann. Phys. **303**, 2 (2003).
[16] J. Zhang, E. G. M. van Kempen, T. Bourdel, L. Khaykovich, J. Cubizolles, F. Chevy, M. Teichmann, L. Tarruell, S. J. J. M. F. Kokkelmans, and C. Salomon, Phys. Rev. A **70**, 030702(R) (2004).
[17] J. P. Gaebler, J. T. Stewart, J. L. Bohn, and D. S. Jin, Phys. Rev. Lett. **98**, 200403 (2007).
[18] J. Fuchs, C. Ticknor, P. Dyke, G. Veeravalli, E. Kuhnle, W. Rowlands, P. Hannaford, and C. J. Vale, Phys. Rev. A **77**, 053616 (2008).
[19] Y. Inada, M. Horikoshi, S. Nakajima, M. Kuwata-Gonokami, M. Ueda, and T. Mukaiyama, Phys. Rev. Lett. **101**, 100401 (2008).
[20] D. S. Petrov, C. Salomon, and G. V. Shlyapnikov, Phys. Rev. A **71**, 012708 (2005).
[21] D. S. Petrov, C. Salomon, and G. V. Shlyapnikov, Phys. Rev. Lett. **93**, 090404 (2004).
[22] J. Levinsen, N. R. Cooper, and V. Gurarie, Phys. Rev. Lett. **99**, 210402 (2007).
[23] M. Jona-Lasinio, L. Pricoupenko, and Y. Castin, Phys. Rev. A **77**, 043611 (2008).
[24] J. Levinsen, Ph.D. thesis, University of Colorado, Boulder, Colorado, 2007.
[25] E. Timmermans, P. Tommasini, M. Hussein, and A. Kerman, Phys. Rep. **315**, 199 (1999).
[26] E. Timmermans, K. Furuya, P. W. Milonni, and A. K. Kerman,

- Phys. Lett. A **285**, 228 (2001).
- [27] M. Holland, S. J. J. M. F. Kokkelmans, M. L. Chiofalo, and R. Walser, Phys. Rev. Lett. **87**, 120406 (2001).
- [28] L. D. Landau and E. M. Lifshitz, *Quantum Mechanics* (Butterworth-Heinemann, Oxford, UK, 1981).
- [29] G. M. Bruun and C. J. Pethick, Phys. Rev. Lett. **92**, 140404 (2004).
- [30] E. Cornell, http://online.itp.ucsb.edu/online/gases_c04/discussion2
- [31] R. Diener and T.-L. Ho, e-print, arXiv:cond-mat/0405174.
- [32] A. V. Andreev, V. Gurarie, and L. Radzihovsky, Phys. Rev. Lett. **93**, 130402 (2004).
- [33] D. S. Petrov, Phys. Rev. Lett. **93**, 143201 (2004).
- [34] H. Suno, B. D. Esry, and C. H. Greene, Phys. Rev. Lett. **90**, 053202 (2003).
- [35] P. Nikolić and S. Sachdev, Phys. Rev. A **75**, 033608 (2007).
- [36] The p -wave two channel model has an additional factor of momentum in its interactions compared to its s -wave counterpart. This changes the power counting effectively replacing d with $d-2$, so that whereas the s -wave two channel model has upper critical dimension $d=4$, the p -wave two channel model's upper critical dimension is $d=2$.
- [37] P. O. Fedichev, M. W. Reynolds, and G. V. Shlyapnikov, Phys. Rev. Lett. **77**, 2921 (1996).
- [38] E. Nielsen and J. H. Macek, Phys. Rev. Lett. **83**, 1566 (1999).
- [39] B. D. Esry, C. H. Greene, and J. P. Burke, Phys. Rev. Lett. **83**, 1751 (1999).
- [40] P. F. Bedaque, E. Braaten, and H.-W. Hammer, Phys. Rev. Lett. **85**, 908 (2000).
- [41] G. V. Skorniakov and K. A. Ter-Martirosian, Zh. Eksp. Teor. Fiz. **31**, 775 (1956) [Sov. Phys. JETP **4**, 648 (1957)].
- [42] P. F. Bedaque, H.-W. Hammer, and U. van Kolck, Nucl. Phys. A **646**, 444 (1999).
- [43] W. H. Press, S. A. Teukolsky, W. T. Vetterling, and B. P. Flannery, *Numerical Recipes in Fortran 77: The Art of Scientific Computing* (Cambridge University Press, Cambridge, 1996).
- [44] D. S. Petrov, M. Holzmann, and G. V. Shlyapnikov, Phys. Rev. Lett. **84**, 2551 (2000).
- [45] D. S. Petrov and G. V. Shlyapnikov, Phys. Rev. A **64**, 012706 (2001).
- [46] M. Olshanii, Phys. Rev. Lett. **81**, 938 (1998).
- [47] L. Pricoupenko, Phys. Rev. Lett. **100**, 170404 (2008).
- [48] N. Syassen, D. M. Bauer, M. Lettner, T. Volz, D. Dietze, J. J. Garcia-Ripoll, J. I. Cirac, G. Rempe, and S. Dürr, Science **320**, 1329 (2008).